Networks and Heterogeneous Media
Vol. 17, No. 5, October 2022, pp. 803–825
doi:10.3934/nhm.2022027

EFFECT OF TIME DELAY ON FLOCKING DYNAMICS

Hyeong-Ohk Bae
Department of Financial Engineering, Ajou University
Republic of Korea

Seung Yeon Cho
Department of Mathematics and Research Institute of Natural Science,
Gyeongsang National University
Republic of Korea

Jane Yoo*
Department of Financial Engineering, Ajou University
Republic of Korea

Seok-Bae Yun
Department of Mathematics, Sungkyunkwan University
Republic of Korea

(Communicated by the Seung-Yeal Ha)

Abstract. We propose a time-delayed Cucker-Smale type model(CS model), which can be applied to modeling (1) collective dynamics of self-propelling agents and (2) the dynamical system of stock return volatility in a financial market. For both models, we assume that it takes a certain amount of time to collect/process information about the current position/return configuration until velocity/volatility adjustment is made. We provide a sufficient condition under which flocking phenomena occur. We also identify the initial configuration for a two-agent case, in which collective behaviors are accelerated by changes in the delay parameter. Numerical illustrations and financial simulations are carried out to verify the validity of the model.

1. **Introduction.** The study of emergent behaviors in particle systems, of which agents interact through uncoordinated and decentralized interaction laws, has seen a surge of interest recently. The emergent phenomena are investigated in various contexts such as flocking - alignment of velocity of self-propelling agents: [17, 20, 24, 39, 46], herding - adjustment of both velocity and position: [4, 6, 7, 40], synchronization - adjustment of oscillation frequency: [1, 29, 47] to name a few.

2020 *Mathematics Subject Classification.* Primary: 82C22, 91B70, 91G80.
Key words and phrases. Cucker–Smale model, flocking, volatility, time delay.
Bae was supported by the Basic Science Research Program through the National Research Foundation of Korea (NRF) funded by the Ministry of Education, Science and Technology (NRF-2021R1A2C1093383), Cho by PRIN Project 2017 (No. 2017KKJP4X entitled "Innovative numerical methods for evolutionary partial differential equations and applications") funded by Italian Ministry of Instruction, University and Research (MIUR), Yoo by Ajou University Research Fund, and Yun by Samsung Science and Technology Foundation under Project Number SSTF-BA1801.
*Corresponding author: Jane Yoo.

The study of the collective dynamics is further diversified by considering various effects such as time delay phenomena [18, 19, 23], randomness [2, 28], connectivity of the underlying graph structure [35], presence of leadership or hierarchy [42], etc.

Among such phenomenological effects, we aim to understand the time delay effect. Since it always takes non-negligible time (or delay) for the information to be transmitted, processed and reflected on agents' behaviors in many real world applications, such delay effects arise ubiquitously in nature, societies, and science: biology [27, 34, 38], physics [44], chemistry [41], engineering [33, 37], finance [32, 45], traffic dynamics [21, 43], and opinion formulation [36].

More precisely, the goal of this paper is to propose a Cucker-Smale type model with time delay, which can be interpreted in the following two ways:

1. As a model to describe the collective dynamics of self-propelling agents, who consider the relative positional configuration over a fixed amount of time to adjust their velocity.
2. As a model to understand the flocking phenomena of multi-asset return volatilities, a measure of uncertainty in a financial market.

As such, our way how to incorporate the delay parameter into a CS model is different from previous CS models with time delay.

After we present the model, we verify sufficient conditions that guarantee collective behaviors of the system, and provide mathematical analysis that captures the effects of delay phenomena on flocking dynamics. That is, we identify the initial configuration that accelerates the flocking phenomena. Our results are distinguished from most results so far provided by the related literature, which focuses on providing sufficient conditions on the delay to guarantee the onset of collective behaviors.

Particularly, our model is developed on the assumption that it takes much shorter for volatility adjustment than returns' adjustment. As such, the way how the delay parameter is incorporated into the model is different from previous CS models with time delay. We verify through numerical simulations that our model is able to forecast real data better than the previous models in the literature.

We organize this paper as follows. In Section 2, we state our modeling assumption and propose a time-delayed CS model. In Section 3, we identify the initial configuration that leads to acceleration of the flocking. In Section 4, the order preservation is discussed. In Section 5, we provide several numerical examples to illustrate the validity of our analytical results. Finally, in Section 6, we discuss the applications of the model in predicting real financial market data.

2. **Modeling time-delayed Cucker-Smale model.**

In this section, we introduce our time-delayed CS model. We also provide motivations of the model from two viewpoints: one from the collective dynamics of self-propelling agents, and the other from volatility flocking phenomena in a financial market.

2.1. **Modeling from the perspectives of self-propelling agents.**

The first motivation comes from the flocking behavior of self-propelling particles. Flocking is about adjusting one's velocity according to the behavior of neighboring particles. Depending on system configuration, such adjustment may occur instantly or may involve a specific time delay. The most common CS type model with time-delay

effect in the literature takes the following form [8, 18, 22]:

$$\begin{aligned} \dot{x}_i^\tau(t) &= v_i^\tau(t), \\ \dot{v}_i^\tau(t) &= \frac{\lambda}{N}\sum_{j=1}^{N}\psi\big(|x_j^\tau(t-\tau)-x_i^\tau(t)|\big)\big(v_j^\tau(t-\tau)-v_i^\tau(t)\big), \end{aligned} \tag{1}$$

where, for each $i = 1, 2, \cdots, N$, $x_i^\tau(t) \in \mathbb{R}$ denotes the position of agent i at time $t \geq -\tau$, and $v_i^\tau(t) \in \mathbb{R}$ denotes the velocity of agent i. We use the supperscript τ to denote their dependence on the delay parameter τ. For the definition of the interaction strength ψ, see [8, 18, 22]. This model corresponds to situations, where a non-negligible time lapse is necessary for information-transmitting from a particle's position and velocity to the others'. We remark that we analyze here the one-dimensional position and velocity. We leave the analysis in a general dimension for future research.

On the other hand, we consider the case, in which it takes some time to collect information about the relative positions of particles until the velocity adjustment with respect to neighboring particles is made. This case is also often found natural. For example, drivers would adjust their speed (either accelerate or slow down) while comparing their relative positions to other cars'. Such comparison is made continuously and necessitates the sufficient amount of time before the instantaneous adjustment is made. A driver keeps accumulating information about his/her neighboring drivers' driving styles and uses the historical data for changing his/her speed when it is necessary. In this situation, the observational time lapse would often be longer than the immediate speed adjustment.

We state our main modeling assumptions in a more rigorous manner as follows:

1. Each agent's velocity is coupled to each other, and their collective dynamics can be described by, among others, a CS type flocking model.
2. The adjustment between velocities of agents occurs immediately, while how intensively they interact to each other depends on the history data of positional configuration.

Assumption (2) can be restated as follows: the time scale for velocity adjustment is negligible compared to the time needed to assess the information about the positions of neighboring agents.

The time-delayed CS model for N agents based on the above assumptions with the delay parameter $\tau > 0$ is given by

$$\mathbf{CS}(\tau): \qquad \begin{cases} \dot{x}_i^\tau = v_i^\tau, \\ \dot{v}_i^\tau = \frac{\lambda}{N}\sum_{j=1}^{N}\Psi_{ij}^\tau\big(v_j^\tau - v_i^\tau\big) \quad \text{for} \quad i = 1, \cdots, N, \\ \big(x_i^\tau(t), v_i^\tau(t)\big) = \big(x_{h,i}^\tau(t), v_{h,i}^\tau(t)\big), \quad -\tau \leq t \leq 0, \end{cases}$$

where $x_i^\tau := x_i^\tau(t)$ and $v_i^\tau := v_i^\tau(t)$. The initial history data $(x_{h,i}^\tau, v_{h,i}^\tau)$ are given functions on the initial time interval $[-\tau, 0]$.

Throughout this paper, we use the following two types of communication functions Ψ_{ij}^τ between agents i and j:

1. Communication function for accumulated historical interaction:

$$\Psi_{ij}^\tau := \Psi\big(x_i^\tau, x_j^\tau, t, \tau\big) := \frac{1}{\tau}\int_{t-\tau}^{t}\psi\big(|x_j^\tau(s) - x_i^\tau(s)|\big)ds. \tag{2}$$

2. Communication function with a fixed delay parameter:

$$\Psi_{ij}^{\tau} := \Psi\big(x_i^{\tau}, x_j^{\tau}, t, \tau\big) := \psi\big(|x_j^{\tau}(t-\tau) - x_i^{\tau}(t-\tau)|\big), \tag{3}$$

with the interaction kernel $\psi(r) : \mathbb{R} \to \mathbb{R}^+$

$$\psi(r) := \frac{1}{(\varepsilon + r^2)^{\frac{\gamma}{2}}}, \qquad (\varepsilon = 1), \tag{4}$$

which is commonly used for describing flocking phenomena in the literature [6, 20, 40, 42]. The interaction strength exponent $\gamma \in \mathbb{R}$ can be derived from assumptions, or can be chosen to fit data. The exponent γ is usually assumed to be non-negative in the study of flocking phenomena between self-propelling agents. (Below, it will be discussed that $\gamma < 0$ is reasonable in models of a financial market.) Note that, when $\varepsilon = 0$ the interaction $\psi(r) = r^{-\gamma}$ becomes singular at $r = 0$ when $\gamma > 0$.

2.2. **Modeling for understanding volatility flocking phenomena in financial markets.** Our second motivation comes from attempts to model stock return volatility flocking phenomena using the delayed interaction between them. For example, in the Generalized Autocorrelated Conditional Heteroskedasticy (GARCH) model [25], a discrete-version of the Stochastic Volatility model [5], the expected volatility at t is represented by the $t-\tau$ observable information set for $0 < \tau \leq t$. By modeling time delay τ, the model can mimic shocks today retaining their influence on volatility and return expectations for many periods in the future.

However, the GARCH model is usually developed as a univariate model, because it is difficult to jointly estimate multivariate volatility dynamics on time. So far, multivariate GARCH or SV model is only developed with strict assumptions [5], [16]. Recently, the CS-type volatility models have advanced the multivariate volatility modeling without loss of computational efficiency. The authors in [9, 10] refer to the CS mechanism, particularly a version that has been applied to explaining the collective behavior in human society [3], [13], and [26]. In [11], various key financial parameters for the CS-type volatility model is calibrated to be referred in its practical use.

More recently, a time-delay CS-type volatility model was suggested in [8], which introduced the delay parameter into the dynamic system of regime switching volatility by following (1). On the other hand, we present a model of multivariate time-delayed CS mechanism based on the following assumptions & observations of volatility dynamics:

1. Asset return volatilities are coupled to each other, and their collective dynamics can be described by, among others, a CS type flocking model.
2. The adjustment between volatilities occurs instantaneously, while how intensively they interact to each other depends on the initial history data of the return.

Assumption (2) would be restated as follows: the time scale for volatilities' adjustment is negligible compared to the time scale for returns' information-exchange. The assumptions will be further discussed and justified through various numerical simulations in Sections 5 and 6.

We assume that N assets are traded in a market. Then, based on the above two assumptions, we derive a time-delayed CS type volatility-flocking model, which takes the exact equation of $\mathbf{CS}(\tau)$. The only difference is about the interpretation: in this context, $x_i^{\tau} := x_i^{\tau}(t)$ denotes the price return of asset i at time $t \geq -\tau$, and

$v_i^\tau := v_i^\tau(t)$ denotes the return's volatility. In this model, a communication noise is not included. Instead, we focus on the time delay effect on the dynamics.

Given no consensus in the literature on which is the appropriate interaction kernel for volatility dynamics modeling, we assume, throughout this paper, that communication functions Ψ_{ij}^τ between agents i and j takes the form (2) or (3) presented above. Contrary to the study of flocking phenomena between self-propelling agents considered in the previous subsection, it is relevant to assume γ to be non-positive. For example, in modeling collective behavior of volatility, it is more reasonable to assume that volatility, which is fluctuating far from others, relaxes faster. This assumption is also consistent with that of [8, 9]. Note that, unlike the self-propelling agents' case, the kernel become degenerate at $r = 0$ when $\varepsilon = 0$ in this case.

3. The effect of time-delay on the flocking dynamics.

In this section, we conduct mathematical analysis of the model **CS**(τ) to understand the qualitative effect caused by such a delay mechanism on flocking dynamics. More precisely, we identify initial configurations under which the time-delay effect can accelerate the overall flocking behavior of the delayed CS model. Our study is unlike most of the results found in mathematical literature on the delay effect in flocking dynamics, focusing on the derivation of sufficient conditions that guarantee the flocking asymptotics in the presence of the delay effect. This analysis is given for the two-particle system. More analyses on systems with a general number of particles are left for the future research.

To state our main results, we define the flocking phenomenon of the system. We start with basic properties of the mean and variance of position and velocity, which are defined as follows:

- means of x^τ and v^τ:

$$x_c^\tau(t) := \frac{1}{N}\sum_{i=1}^N x_i^\tau(t), \quad v_c^\tau(t) := \frac{1}{N}\sum_{i=1}^N v_i^\tau(t).$$

- variances of x^τ and v^τ:

$$\mathcal{X}_\tau(t) := \frac{1}{N}\sum_{i=1}^N |x_i^\tau(t) - x_c^\tau(t)|^2, \quad \mathcal{V}_\tau(t) := \frac{1}{N}\sum_{i=1}^N |v_i^\tau(t) - v_c^\tau(t)|^2.$$

Lemma 3.1. *Let (x^τ, v^τ) be the solution to **CS**(τ). If the initial data is given by*

$$x_c^\tau(0) = v_c^\tau(0) = 0, \tag{5}$$

then we have $x_c^\tau(t) = v_c^\tau(t) = 0$ for all $t > 0$.

Proof. Due to the symmetry of $\Psi_{ij}^\tau = \Psi_{ji}^\tau$, we have

$$\dot{v}_c^\tau = \frac{\lambda}{N^2}\sum_{i=1}^N\sum_{j=1}^N \Psi_{ij}^\tau\big(v_j^\tau - v_i^\tau\big) = 0.$$

This, together with (5), gives the desired result. □

In view of Lemma 3.1, we fix x_c^τ and v_c^τ for our convenience.

We summarize our assumptions that are applied throughout the paper.

- We assume $\varepsilon = 1$ and $\gamma > 0$ for the communication function (4).
- We assume $x_c^\tau(0) = v_c^\tau(0) = 0$.

Under these assumptions, the flocking phenomena of the system $\mathbf{CS}(\tau)$ is defined more succinctly as follows:

Definition 3.2. Let (x^τ, v^τ) be the solution to $\mathbf{CS}(\tau)$. We say the *asymptotic flocking* occurs if

$$\lim_{t\to+\infty} |v_i^\tau(t)| = 0, \quad \text{and} \quad \max_{1\le i\le N} |x_i^\tau(t)| < \infty \qquad \text{for } i = 1, 2, \cdots, N.$$

Now, we are ready to state our main theoretical result, which compares the decay speed of system $\mathbf{CS}(\tau)$ corresponding respectively to delays parameters $\tau_2 > \tau_1 > 0$.

Theorem 3.3. *Let $N = 2$. Fix $\tau_2 > \tau_1 \ge 0$. Let (x^{τ_2}, v^{τ_2}) and (x^{τ_1}, v^{τ_1}) be the solutions to $\mathbf{CS}(\tau_2)$ and $\mathbf{CS}(\tau_1)$, respectively, for the interaction kernel (4) with $\varepsilon > 0$. Assume the following ordering condition holds for $t \in [-\tau_2, 0]$:*

$$\begin{aligned} &x_{h,1}^{\tau_2}(t) < x_{h,2}^{\tau_2}(t), \quad v_{h,1}^{\tau_2}(t) < v_{h,2}^{\tau_2}, \quad \text{for } t \in [-\tau_2, 0], \\ &x_h^{\tau_1}(t) = x_h^{\tau_2}(t), \quad v_h^{\tau_1}(t) = v_h^{\tau_2}(t), \quad \text{for } t \in [-\tau_1, 0], \end{aligned} \tag{6}$$

where $x_h^\tau := \left(x_{h,1}^\tau, x_{h,2}^\tau, ..., x_{h,N}^\tau\right)$ and $v_h^\tau := \left(v_{h,1}^\tau, v_{h,2}^\tau, ..., v_{h,N}^\tau\right)$ for given τ. Then, we have for $t > 0$,

$$\mathcal{V}_{\tau_2}(t) < \mathcal{V}_{\tau_1}(t),$$

where $\mathcal{V}_{\tau_1}(t) = \frac{1}{N}\sum_{i=1}^N |v_i^{\tau_1}(t)|^2$ and $\mathcal{V}_{\tau_2}(t) = \frac{1}{N}\sum_{i=1}^N |v_i^{\tau_2}(t)|^2$ are the variances of the velocities to $\mathbf{CS}(\tau_1)$ and $\mathbf{CS}(\tau_2)$ with zero means, respectively.

3.1. **Range of γ for flocking.** We show that asymptotic flocking occurs to our problem $\mathbf{CS}(\tau)$ at least when $\gamma \in [0, 1]$.

Lemma 3.4. *Let (x^τ, v^τ) be the solution to $\mathbf{CS}(\tau)$. Given $\tau \ge 0$, the energy functional $\mathcal{X}_\tau$ and $\mathcal{V}_\tau$ satisfies*

$$\mathcal{V}_\tau(t) \le \mathcal{V}_\tau(0) e^{-2\lambda \int_0^t \Psi_{\min}^\tau(s)\, ds}, \qquad \mathcal{X}_\tau(t) \le 2\left(\mathcal{X}_\tau(0) + \mathcal{V}_\tau(0) t^2\right).$$

Proof. From Lemma 3.1, we set $x_c^\tau \equiv v_c^\tau \equiv 0$. Then,

$$\frac{d\mathcal{V}_\tau(t)}{dt} = -\frac{\lambda}{N^2}\sum_{i=1}^N\sum_{j=1}^N \Psi_{ij}^\tau |v_j^\tau(t) - v_i^\tau(t)|^2 \le -2\lambda \Psi_{\min}^{\tau(t)} \mathcal{V}_\tau(t),$$

which yields $\mathcal{V}_\tau(t) \le \mathcal{V}_\tau(0) e^{-2\lambda \int_0^t \Psi_{\min}^\tau(s)\, ds}$.

For $\mathcal{X}_\tau$, we obtain the following inequality:

$$\begin{aligned} \frac{d\mathcal{X}_\tau(t)}{dt} &= \frac{2}{N}\sum_{i=1}^N x_i^\tau(t) v_i^\tau(t) \le 2\sqrt{\mathcal{X}_\tau(t)}\sqrt{\mathcal{V}_\tau(t)} \\ &\le 2\sqrt{\mathcal{V}_\tau(0)} e^{-\lambda \int_0^t \Psi_{\min}^\tau(s)\, ds} \sqrt{\mathcal{X}_\tau(t)}. \end{aligned}$$

Solving this, we have

$$\sqrt{\mathcal{X}_\tau(t)} - \sqrt{\mathcal{X}_\tau(0)} \le \sqrt{\mathcal{V}_\tau(0)} \int_0^t e^{-\lambda \int_0^s \Psi_{\min}^\tau(u)\, du}\, ds,$$

and hence we obtain our result, where the minimum of the interaction kernel is defined by

$$\Psi_{\min}^\tau(t) := \min_{1\le i,j\le N} \Psi_{ij}^\tau(t).$$

□

In the following proposition, we show that asymptotic flocking occurs when $\gamma \in [0,1]$.

Proposition 1. *Let (x^τ, v^τ) be the solution to* **CS**(τ). *Given $\tau \geq 0$, we have*

$$\lim_{t\to+\infty} \int_0^t \Psi_{\min}^\tau(s)ds = \infty$$

for $\gamma \in [0,1]$.

Proof. From Lemma 3.4, we have

$$|x_i^\tau(s) - x_j^\tau(s)|^2 \leq 2N\mathcal{X}_\tau(s) \leq \max\left\{2N\left(\mathcal{X}_\tau(0) + \mathcal{V}_\tau(0)t^2\right), \sup_{-\tau\leq u\leq 0} 2N\mathcal{X}_\tau(u)\right\}$$

for $t-\tau \leq s \leq t$. Then, this gives

$$\begin{aligned}
\Psi_{\min}^\tau(t) &\geq \min_{1\leq i,j\leq N}\left\{\inf_{t-\tau\leq s\leq t} \psi\big(|x_i^\tau(s) - x_j^\tau(s)|\big)\right\} \\
&\geq \psi\left(\left|\max\left\{2N\big(\mathcal{X}_\tau(0) + \mathcal{V}_\tau(0)t^2\big), \sup_{-\tau\leq u\leq 0} 2N\mathcal{X}_\tau(u)\right\}\right|^{\frac{1}{2}}\right) \\
&\geq \left(\frac{1}{1+\sup_{-\tau\leq u\leq 0} 2N\mathcal{X}_\tau(u) + 2N\mathcal{V}_\tau(0)}\right)^{\frac{\gamma}{2}} \frac{1}{(1+t^2)^{\frac{\gamma}{2}}} \\
&\geq \frac{\kappa}{(1+t)^\gamma},
\end{aligned}$$

where $\kappa := \big(1+\sup_{-\tau\leq u\leq 0} 2N\mathcal{X}_\tau(u) + 2N\mathcal{V}_\tau(0)\big)^{-\frac{\gamma}{2}}$. Then, the desired result follows from $0 \leq \gamma \leq 1$. □

3.2. **Proof of theorem 3.3.** We first show that the sign of velocity v_i^τ, $i = 1, 2$, does not change as time goes on.

Lemma 3.5. *Given $\tau > 0$, let (x, v) be the solution to* **CS**(τ). *For $N = 2$, if we have*

$$v_{h,1}^\tau(0) < 0 < v_{h,2}^\tau(0), \tag{7}$$

this inequality holds for all $t > 0$.

Proof. The relation $x_c = v_c \equiv 0$ gives

$$\dot{x}_2^\tau = v_2^\tau, \qquad \dot{v}_2^\tau = -\lambda\Psi_{21}^\tau v_2^\tau.$$

Here, Ψ_{21}^τ is either $\Psi_{21}^\tau = \frac{1}{\tau}\int_{t-\tau}^t \psi\big(|2x_2^\tau(s)|\big)ds$ or $\Psi_{21}^\tau = \psi\big(|2x_2(t-\tau)|\big)$. Then, we have

$$v_2^\tau = v_2^\tau(0)e^{-\lambda\int_0^t \Psi_{21}^\tau(s)\,ds} > 0,$$

and this together with the assumption (7) gives the desired result. □

Proof of Theorem 3.3. For $N = 2$, under the condition (6), we have $\mathcal{V}_{\tau_2}(0) = \mathcal{V}_{\tau_1}(0)$ and

$$\begin{aligned}
\mathcal{V}'_{\tau_2}(0) &= -\frac{\lambda}{N^2}\sum_{i=1}^N\sum_{j=1}^N \Psi_{ij}^{\tau_2}\big|v_{h,j}^{\tau_2}(0) - v_{h,i}^{\tau_2}(0)\big|^2 \\
&< -\frac{\lambda}{N^2}\sum_{i=1}^N\sum_{j=1}^N \Psi_{ij}^{\tau_1}\big|v_{h,j}^{\tau_1}(0) - v_{h,i}^{\tau_1}(0)\big|^2 \\
&= \mathcal{V}'_{\tau_1}(0) < 0.
\end{aligned} \tag{8}$$

Suppose, to the contrary, that $\mathcal{V}_{\tau_1}$ and $\mathcal{V}_{\tau_2}$ become identical at a first time $t^* > 0$, that is,

$$\mathcal{V}_{\tau_2}(t^*) = \mathcal{V}_{\tau_1}(t^*) \quad \text{and} \quad \mathcal{V}_{\tau_2}(t) \neq \mathcal{V}_{\tau_1}(t) \ \text{ for } 0 < t < t^*. \tag{9}$$

Here, we note that the relation $v_c^{\tau_2} = v_c^{\tau_1} = 0$ implies

$$\mathcal{V}_{\tau_2}(t) = \left|v_2^{\tau_2}(t)\right|^2, \quad \mathcal{V}_{\tau_1}(t) = \left|v_2^{\tau_1}(t)\right|^2,$$

and hence (8) gives

$$|v_2^{\tau_2}|^2 < |v_2^{\tau_1}|^2$$

for $0 < t < t^*$. Furthermore, Lemma 3.5 says that the sign of $v_2^{\tau_2}$ and $v_2^{\tau_1}$ will not change for $t > 0$. Therefore,

$$0 < v_2^{\tau_2} < v_2^{\tau_1} \tag{10}$$

for $0 < t < t^*$. Then, this also implies that for $0 < t < t^*$,

$$0 < x_2^{\tau_2} < x_2^{\tau_1}. \tag{11}$$

Now, we claim that the following inequality holds, for any $t \in (0, t^*)$,

$$\Psi\big(x_1^{\tau_2}, x_2^{\tau_2}, t, \tau_2\big) > \Psi\big(x_1^{\tau_1}, x_2^{\tau_1}, t, \tau_1\big).$$

For this, we separate the proof into two cases depending on the choice of Ψ: (2) and (3).

• **Case of (2):** For $0 < t < t^*$, we have from (10) that $x_2^{\tau_2}$ and $x_2^{\tau_1}$ are increasing functions of t. Then the relation (11) gives

$$\begin{aligned}
\frac{1}{\tau_2}\int_{t-\tau_2}^{t} \psi(|2x_2^{\tau_2}(s)|)ds &= \frac{1}{\tau_2}\int_{t-\tau_1}^{t} \psi\big(|2x_2^{\tau_2}(s)|\big)ds + \frac{1}{\tau_2}\int_{t-\tau_2}^{t-\tau_1} \psi\big(|2x_2^{\tau_2}(s)|\big)ds \\
&> \frac{1}{\tau_2}\int_{t-\tau_1}^{t} \psi\big(|2x_2^{\tau_1}(s)|\big)ds + \frac{1}{\tau_2}\int_{t-\tau_2}^{t-\tau_1} \psi\big(|2x_2^{\tau_1}(s)|\big)ds \\
&> \frac{1}{\tau_2}\int_{t-\tau_1}^{t} \psi\big(|2x_2^{\tau_1}(s)|\big)ds + \frac{\tau_2-\tau_1}{\tau_2}\psi\big(|2x_2^{\tau_1}(t-\tau_1)|\big) \\
&> \frac{1}{\tau_2}\int_{t-\tau_1}^{t} \psi\big(|2x_2^{\tau_1}(s)|\big)ds \\
&\quad + \left(1-\frac{\tau_1}{\tau_2}\right)\frac{1}{\tau_1}\int_{t-\tau_1}^{t} \psi\big(|2x_2^{\tau_1}(s)|\big)ds \\
&= \frac{1}{\tau_1}\int_{t-\tau_1}^{t} \psi\big(|2x_2^{\tau_1}(s)|\big)ds.
\end{aligned}$$

• **Case of (3):** For $0 < t < t^*$, it suffices to show

$$x_2^{\tau_2}(t-\tau_2) < x_2^{\tau_1}(t-\tau_1). \tag{12}$$

We first consider the case $t-\tau_2 < t-\tau_1 \le 0$. Since the condition (6) implies $v_2 > 0$ for $t \le 0$, we have

$$\begin{aligned} x_2^{\tau_2}(t-\tau_2) &= x_2^{\tau_2}(-\tau_2) + \int_{-\tau_2}^{t-\tau_2} v_2^{\tau_2}(s)ds \\ &= x_2^{\tau_1}(-\tau_2) + \int_{-\tau_2}^{t-\tau_2} v_2^{\tau_1}(s)ds \\ &< x_2^{\tau_1}(-\tau_2) + \int_{-\tau_2}^{t-\tau_1} v_2^{\tau_1}(s)ds = x_2^{\tau_1}(t-\tau_1). \end{aligned}$$

When $t-\tau_2 \le 0 < t-\tau_1$,

$$x_2^{\tau_2}(t-\tau_2) < x_2^{\tau_2}(0) = x_2^{\tau_1}(0) < x_2^{\tau_1}(t-\tau_1).$$

When $0 < t-\tau_2 < t-\tau_1$,

$$\begin{aligned} x_2^{\tau_2}(t-\tau_2) &= x_2^{\tau_2}(0) + \int_0^{t-\tau_2} v_2^{\tau_2}(s)ds \\ &< x_2^{\tau_1}(0) + \int_0^{t-\tau_2} v_2^{\tau_1}(s)ds \\ &< x_2^{\tau_1}(0) + \int_0^{t-\tau_2} v_2^{\tau_1}(s)ds + \int_{t-\tau_2}^{t-\tau_1} v_2^{\tau_1}(s)ds \\ &= x_2^{\tau_1}(t-\tau_1). \end{aligned}$$

Now, the claim (12) implies that the following inequality holds for all $0 < t < t^*$:

$$\psi(\|2x_2^{\tau_2}(t-\tau_2)\|) > \psi(\|2x_2^{\tau_1}(t-\tau_1)\|).$$

In both cases, we have

$$\mathcal{V}'_{\tau_2}(t) = -2\lambda\mathcal{V}_{\tau_2}\Psi\big(x_1^{\tau_2}, x_2^{\tau_2}, t, \tau_2\big), \quad \mathcal{V}'_{\tau_1}(t) = -2\lambda\mathcal{V}_{\tau_1}(t)\Psi\big(x_1^{\tau_1}, x_2^{\tau_1}, t, \tau_1\big).$$

Consequently, we obtain the following inequality:

$$\begin{aligned} \mathcal{V}_{\tau_2}(t^*) &= \mathcal{V}_{\tau_2}(0)e^{-2\lambda\int_0^{t^*}\Psi\left(x_1^{\tau_2}, x_2^{\tau_2}, t, \tau_2\right)dt} \\ &< \mathcal{V}_{\tau_1}(0)e^{-2\lambda\int_0^{t^*}\Psi\left(x_1^{\tau_1}, x_2^{\tau_1}, t, \tau_1\right)dt} = \mathcal{V}_{\tau_1}(t^*), \end{aligned}$$

which contradicts (9). □

4. **Order preservation.** In this section, we show that the order preserving property holds for our model. The number of agents are not restricted. We first show that the flocking does not occur in finite time:

Lemma 4.1. *Given $\tau \ge 0$, let (x^τ, v^τ) be the solution to* **CS**(τ). *Suppose that we have initial data with $\mathcal{V}_\tau(0) > 0$. Then, all of $\{v_i^\tau\}_{i=1}^N$ are not identical in finite time.*

Proof. Recalling $v_c \equiv 0$, we get

$$\frac{d\mathcal{V}_\tau}{dt} = \frac{d}{dt}\left\{\frac{1}{N}\sum_{i=1}^N |v_i^\tau|^2\right\} = -\frac{\lambda}{N^2}\sum_{i=1}^N\sum_{j=1}^N \Psi_{ij}^\tau |v_j^\tau - v_i^\tau|^2.$$

Now, we use $\psi \le \psi_\infty$ to get

$$\frac{d\mathcal{V}_\tau}{dt} \ge -\frac{\lambda}{N^2}\sum_{i=1}^N\sum_{j=1}^N \psi_\infty |v_j^\tau - v_i^\tau|^2 = -2\lambda\psi_\infty\mathcal{V}_\tau.$$

This implies that $\mathcal{V}_\tau$ is not zero at finite time if $\mathcal{V}_\tau(0) > 0$. □

Next, we show that the positions of any two agents cannot be overlapped before their velocities are completely aligned.

Lemma 4.2. *Let (x^τ, v^τ) be the solution to* **CS**(τ)*. Given $\tau \geq 0$, assume that the following condition holds for $t \in [-\tau, 0]$:*

$$x^\tau_{h,1}(t) < x^\tau_{h,2}(t) < \cdots < x^\tau_{h,N}(t), \quad v^\tau_{h,1}(t) < v^\tau_{h,2}(t) < \cdots < v^\tau_{h,N}(t). \tag{13}$$

If any pair of (x^τ_i, x^τ_j) becomes identical in finite time $T > 0$, there exists $0 < t^* < T$ such that $v^\tau_i(t^*) = v^\tau_j(t^*)$.

Proof. Suppose that there exists a pair of indices (i, j) such that

$$x^\tau_i(T) = x^\tau_j(T), \quad i < j.$$

Then, we consider

$$x^\tau_j(T) - x^\tau_i(T) = x^\tau_j(0) - x^\tau_i(0) + \int_0^T \left\{v^\tau_j(s) - v^\tau_i(s)\right\} ds.$$

Recalling (13), we know

$$x^\tau_j(0) - x^\tau_i(0) > 0,$$

which gives

$$\int_0^T \left\{v^\tau_j(s) - v^\tau_i(s)\right\} ds < 0. \tag{14}$$

If the equality $v^\tau_i = v^\tau_j$ does not occur within interval $[0, T]$, the continuity of v^τ_i and v^τ_j, and the initial condition $0 < v^\tau_j(0) - v^\tau_i(0)$ imply

$$\int_0^T \left\{v^\tau_j(s) - v^\tau_i(s)\right\} ds > 0.$$

This contradicts (14). □

In the following lemma, we consider the first time when a pair $i < j$ violates the condition (13), and observe the behavior of v_k, where $i \leq k \leq j$:

Lemma 4.3. *Let (x^τ, v^τ) be the solution to* **CS**(τ)*. Given $\tau \geq 0$, assume that the condition (13) holds for $t \in [-\tau, 0]$. Suppose a pair v^τ_i, v^τ_j $(i < j)$ violates (13) for the first time at $t = t^*$, that is, t^* is the minimum time with $v^\tau_i(t^*) = v^\tau_j(t^*)$. Then, we have*

$$v^\tau_i(t^*) = v^\tau_k(t^*) = v^\tau_j(t^*), \quad \forall k \in \{i, i+1, \cdots, j-1, j\}.$$

Proof. Suppose, to the contrary, that there exists an index $k \in \{i+1, \cdots, j-1\}$ such that

$$v^\tau_i(t^*) = v^\tau_j(t^*) \neq v^\tau_k(t^*).$$

Without loss of generality, we assume

$$v^\tau_i(t^*) = v^\tau_j(t^*) < v^\tau_k(t^*).$$

Then, since we have from (13) that

$$v^\tau_k(0) < v^\tau_j(0),$$

the intermediate value theorem implies that there exists $t^{**} < t^*$ such that

$$v^\tau_j(t^{**}) = v^\tau_k(t^{**}).$$

This contradicts the assumption that t^* is the first time when the condition (13) is violated. □

Proposition 2. *Let (x^τ, v^τ) be the solution to* **CS**(τ). *Given $\tau \geq 0$, if the following condition holds for $t \in [-\tau, 0]$:*

$$x^\tau_{h,1}(t) < x^\tau_{h,2}(t) < \cdots < x^\tau_{h,N}(t), \quad v^\tau_{h,1}(t) < v^\tau_{h,2}(t) < \cdots < v^\tau_{h,N}(t). \tag{15}$$

Then, this ordering is preserved for $t \geq 0$:

$$x^\tau_1(t) < x^\tau_2(t) < \cdots < x^\tau_N(t), \quad v^\tau_1(t) < v^\tau_2(t) < \cdots < v^\tau_N(t).$$

Proof. Suppose that the condition (15) is first violated at time $t^* > 0$. Then, due to Lemmas 4.2 and 4.3, there exists an index $i \in \{1, 2, \cdots, N-1\}$ such that

$$v^\tau_{i+1}(t^*) = v^\tau_i(t^*) =: \mathrm{v},$$

and

$$\begin{cases} v^\tau_j(t^*) - \mathrm{v} \geq 0, & \forall j \geq i+1 \\ v^\tau_j(t^*) - \mathrm{v} \leq 0, & \forall j \leq i \end{cases}. \tag{16}$$

Note that Lemma 4.1 guarantees the existence of an index k such that

$$v^\tau_k(t^*) \neq \mathrm{v}.$$

Since the condition (15) is violated first at t^*, Lemma 4.2 implies that the following relation holds at t^*:

$$x^\tau_{j+1}(t^*) > x^\tau_j(t^*), \quad \forall j \in \{1, 2, \cdots, N-1\},$$

which implies that

$$\begin{cases} \psi\big(\|x^\tau_j(t^*-\tau) - x^\tau_{i+1}(t^*-\tau)\|\big) > \psi\big(\|x^\tau_j(t^*-\tau) - x^\tau_i(t^*-\tau)\|\big), & \forall j > i+1 \\ \psi\big(\|x^\tau_j(t^*-\tau) - x^\tau_{i+1}(t^*-\tau)\|\big) < \psi\big(\|x^\tau_j(t^*-\tau) - x^\tau_i(t^*-\tau)\|\big), & \forall j < i \end{cases}. \tag{17}$$

From (16) and (17), we find that

$$\begin{aligned} &\dot v^\tau_{i+1}(t^*) - \dot v^\tau_i(t^*) \\ &= \frac{\lambda}{N}\sum_{j=1}^N \Psi^\tau_{i+1,j}(t^*)\big(v^\tau_j(t^*) - v^\tau_{i+1}(t^*)\big) - \frac{\lambda}{N}\sum_{j=1}^N \Psi^\tau_{i,j}(t^*)\big(v^\tau_j(t^*) - v^\tau_i(t^*)\big) \\ &= \frac{\lambda}{N}\sum_{j=i+2}^N \Big(\Psi^\tau_{i+1,j}(t^*) - \Psi^\tau_{i,j}(t^*)\Big)\big(v^\tau_j(t^*) - \mathrm{v}\big) \\ &+ \frac{\lambda}{N}\sum_{j=1}^{i-1} \Big(\Psi^\tau_{i+1,j}(t^*) - \Psi^\tau_{i,j}(t^*)\Big)\big(v^\tau_j(t^*) - \mathrm{v}\big) \\ &> 0. \end{aligned}$$

Therefore, by the continuity of $v_{i+1} - v_i$, there exists a time $0 < t^{**} < t^*$ for which we have

$$v^\tau_{i+1}(t^{**}) - v^\tau_i(t^{**}) < 0.$$

But, considering $v^\tau_{i+1}(0) - v^\tau_i(0) > 0$, this implies that

$$v^\tau_{i+1}(t^{***}) - v^\tau_i(t^{***}) = 0$$

for some $0 < t^{***} < t^{**}$. This contradicts the assumption that t^* is the first time for which $v_{i+1}^\tau(t^*) - v_i^\tau(t^*) = 0$. This completes the proof. □

5. **Numerical simulation.** We now present several numerical examples using the model **CS**(τ). First, we conduct numerical simulation to verify the result in Theorem 3.3. We also conduct a simulation with history data that violate condition (6). Second, we examine simulations related with Proposition 2. This examination provides an insight for understanding the time delay's effects on the flocking speed of agents $N > 2$. For numerical experiments, we use the Euler scheme with fixed time step $\Delta t = 1/128$. In each test, we set history data according to the solutions to **CS**(0) for $t \in [-2, 0]$, i.e.,

$$x_h^\tau(t) := x_h^0(t), \quad v_h^\tau(t) := v_h^0(t), \quad t \in [-2, 0].$$

5.1. **Case** $N = 2$**.** By Theorem 3.3, we show that different variances' decaying speed made by different time delay are subject to the configuration of history data. To confirm it, we conduct the numerical analysis for comparing the time evolution of variances with various time delays in **CS**(τ).

5.1.1. *Verification of theorem 3.3.* According to Theorem 3.3, given two different time delays, if history data satisfy the order condition (6), faster flocking behaviors arise with larger time delays. This tendency is found by examining the flocking behavior with increasing values of time-delays $\tau = 0, \frac{1}{4}, \frac{1}{2}, 1, \frac{5}{4}, \frac{3}{2}$. For this experiment, we consider $\gamma = 1, \lambda = 1$, and take history data for $t \in [-2, 0]$ by the solution to **CS**(0) with initial data,

$$x_{h,1}^0(-2) = -1, \ x_{h,2}^0(-2) = 1, \quad v_{h,1}^0(-2) = -1, \ v_{h,2}^0(-2) = 1.$$

Then, the initial data satisfy the condition (6), because Proposition 2 holds for $\tau = 0$.

In Figure 1, we depict the time evolution of x^τ, v^τ and $\mathcal{V}_\tau$ up to $t = 18$. Separate numerical simulations are conducted for different communication functions. Each experiment's results are found in the left(with (2)) and right(with (3)) panel, respectively. We find no solutions crossing out, implying that the order of solution is preserved. Furthermore, in Figures 1e-1f, we observe that $\mathcal{V}_\tau$ converges to zero rapidly as τ increases. The difference between solutions by different delays with the kernel (2) is smaller than that with the kernel (3).

5.1.2. *Violation of condition* (6). For better understanding the role of initial configurations in Theorem 3.3, here we consider history data which violate the condition (6). As in Section 5.1.1, we take $\gamma = 1, \lambda = 1$ and prepare history data by solving **CS**(0) with

$$x_{h,1}^0(-2) = -6, \ x_{h,2}^0(-2) = 6, \quad v_{h,1}^0(-2) = 1, \ v_{h,2}^0(-2) = -1.$$

Here, the values of $x_{h,1}^0(-2)$ and $x_{h,2}^0(-2)$ are set to be relatively far from each other (compared to Section 5.1.1) to compare the flocking speed without considering any collision between solutions for each τ. In Figure 2, the trajectory of x^τ and v^τ shows no collision for each fixed time delay τ. Particularly, in Figures 2e–2f, we confirm that the variance $\mathcal{V}_\tau$ corresponding to a smaller time delay shows a more pronounced decreasing tendency before the time interval $[9, 10]$. This pattern is contrary to the results in Theorem 3.3. However, after the time interval, it appears that variances corresponding to larger time delays decay faster. Consistent results are obtained for two interaction kernels (2) and (3). As observed in Section 5.1.1,

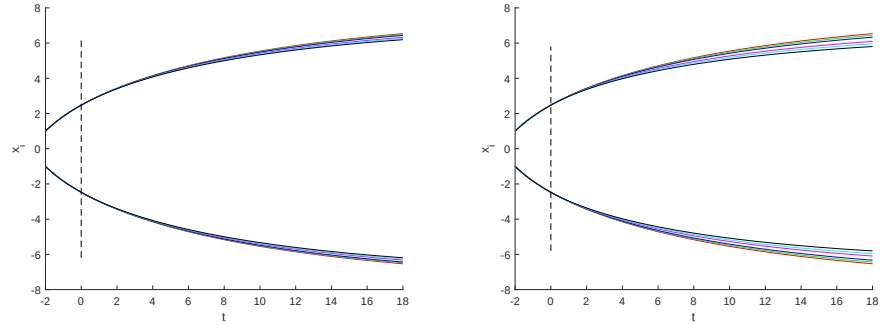

(A) Position x_i^τ with (2)

(B) Position x_i^τ with (3)

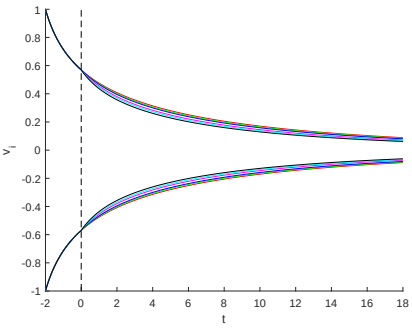

(C) Velocity v_i^τ with (2)

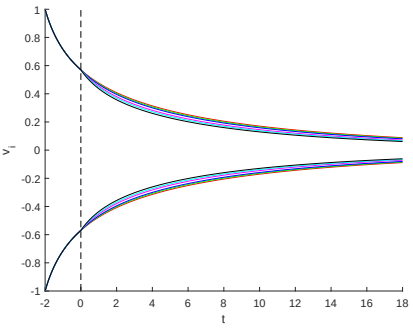

(D) Velocity v_i^τ with (3)

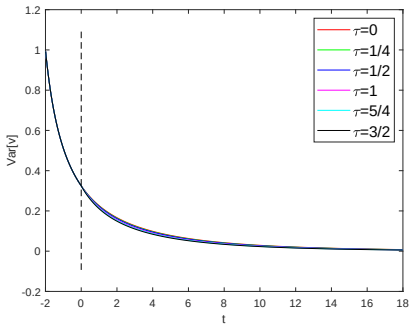

(E) Variance $\mathcal{V}_\tau$ with (2)

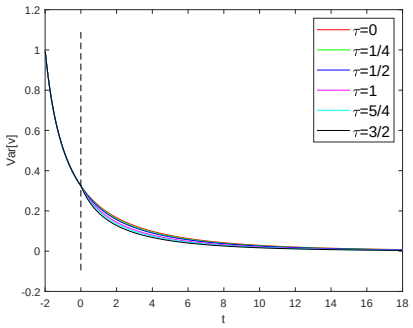

(F) Variance $\mathcal{V}_\tau$ with (3)

FIGURE 1. Verification of Theorem 3.3: Time evolution of position(top), velcocity(middle) and variance(bottom) with two types of communication (2)(left) and (3)(right). Each line show the results with various time delays. History data and other parameter values are given in Section 5.1.1.

the averaged interaction kernel (2) shows smaller differences between results with different delays.

5.2. **Case $N = 3$.** In Proposition 2, we show that the ordering relation (15) maintains for all $t \geq 0$. Here, we verify this property for $N = 3$ and then show the

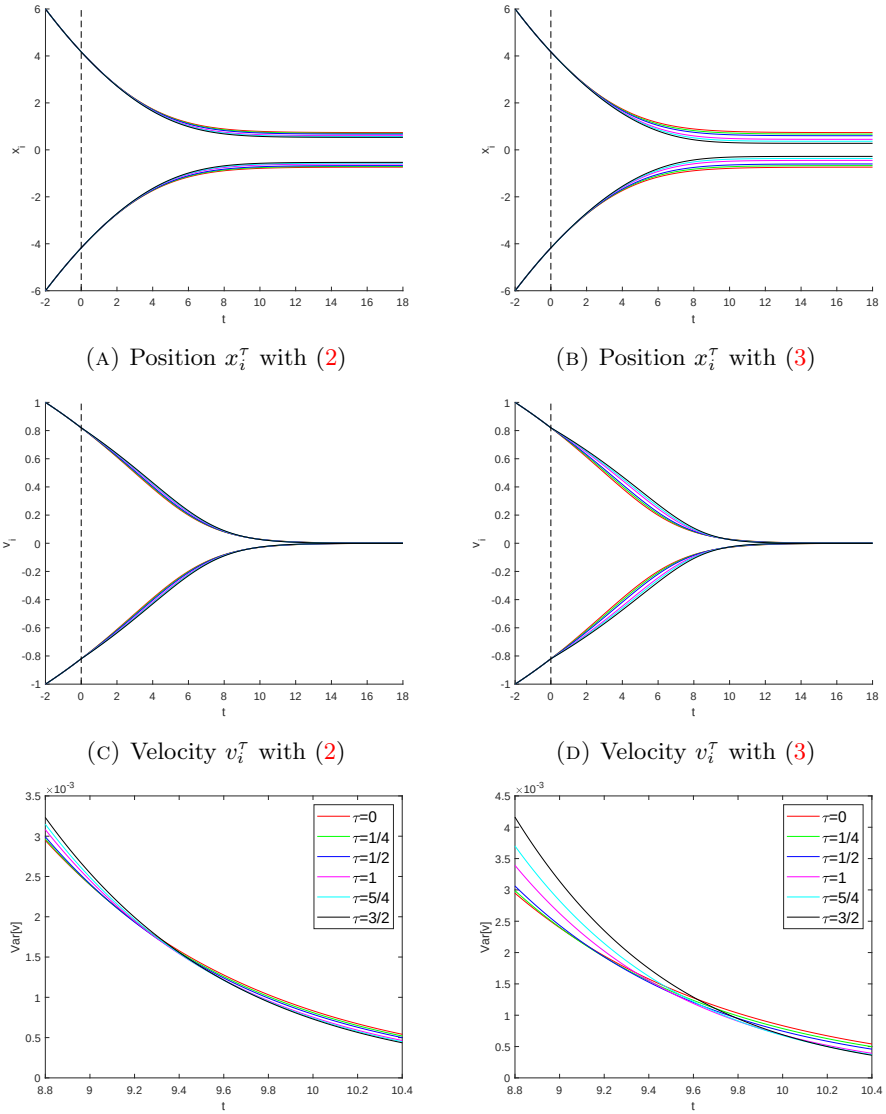

(A) Position x_i^τ with (2)

(B) Position x_i^τ with (3)

(C) Velocity v_i^τ with (2)

(D) Velocity v_i^τ with (3)

(E) Variance $\mathcal{V}_\tau$ with (2)

(F) Variance $\mathcal{V}_\tau$ with (3)

FIGURE 2. Violation of condition (6): Time evolution of position(top), velcocity(middle) and variance(bottom) with two types of communication (2)(left) and (3)(right). Each line show the results with various time delays. History data and other parameter values are given in Section 5.1.2.

effects of different time delays on the flocking behaviors. For the experiments, we use $\gamma = 1, \lambda = 1$ and history data from $t = -2$ to $t = 0$ by the solution of **CS**(0) with initial data,

$$\begin{aligned} x^0_{h,1}(-2) &= 3.719443170061712, & v^0_{h,1}(-2) &= -3.689068693043051, \\ x^0_{h,2}(-2) &= -8.764952796300973, & v^0_{h,2}(-2) &= -6.007401634608296, \\ x^0_{h,3}(-2) &= 5.045509626239265, & v^0_{h,3}(-2) &= 9.696470327651342. \end{aligned} \tag{18}$$

From Figure 3, it is noteworthy to find that solutions maintain the ordering condition (15) for $t \geq 0$. Moreover, the result from the $N = 3$ case also shows that larger time delays lead to faster flocking tendency. Although we do not report the numerical results for larger values of N, we also observed that larger time delays led to faster flocking behaviors for ordered history data satisfying (15). From this numerical observations, we expect Theorem 3.3 to be generalized to the case $N > 2$.

Although our theoretical results are found for $\gamma \geq 0$, we provide numerical results about the solutions' behavior with $\gamma < 0$ regarding the interaction between asset return volatilities as mentioned in Section 2. We reuse the history data of the previous simulations and set $\gamma = -1$, and $\lambda = 0.004$. In Figure 4, we show that when the order condition is not preserved, the time delay effect is reversed to show decelerated flocking with a larger time delay.

Finally, we study the case that the order relation (15) is violated for $N = 3$. We prepare for history data by solving the problem **CS**(0) with initial data

$$\begin{aligned} x^0_{h,1}(-2) &= -16.276445076710459, & v^0_{h,1}(-2) &= -0.635594737301151, \\ x^0_{h,2}(-2) &= 3.200093962187581, & v^0_{h,2}(-2) &= -5.263727976621469, \\ x^0_{h,3}(-2) &= 13.076351114522879, & v^0_{h,3}(-2) &= 5.899322713922622. \end{aligned} \tag{19}$$

From Figure 5, we find that the solutions are crossing-out as t develops. Thus, the flocking speed is not monotonically changing(increasing or decreasing) by the increase in the time delay. Although we report the results based on two initial data (18), satisfying (15), and (19), violating (15), consistent results are found from simulations with other history data.

6. **Applications in financial market data.** The aim of this section is twofold. First, we provide details about how to apply Model **CS**(τ) to study financial data. By providing details, we discuss the model's power of explaining the stylized facts about stock returns' volatilities such as volatility clustering and comovement. Second, we discuss the model's predicting power. We compare our model's predicting power with that of the efficient market hypothesis (EMH), a classical finance theory in predicting the value at $t+1$. According to EMH, the best prediction of tomorrow expectation $\mathbb{E}[x_{t+1}]$ is today's realization x_t because the market is fully efficient for the current price reflect all available information for market participants. Thus, any difference between realized x_{t+1} and x_t is stochastic shocks ε_{t+1} that are not predictable at t. Finally, we also compare the model's predicting power with a popularly used time-delayed CS type model in predicting the dynamics of stock return volatility.

Here, we consider the dynamics of asset i's log price $dS_i(t)/S_i(t)$:

$$\frac{dS_i(t)}{S_i(t)} = x_i(t)dt + v_i(t)dW_i(t), \quad t > 0, \quad 1 \leq i \leq N, \tag{20}$$

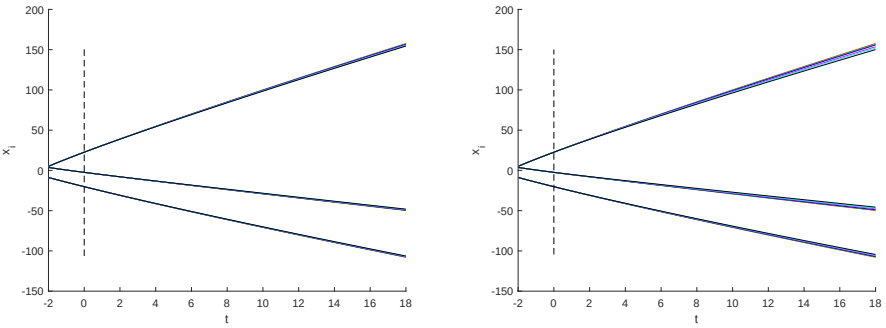

(A) Position x_i^τ with (2)

(B) Position x_i^τ with (3)

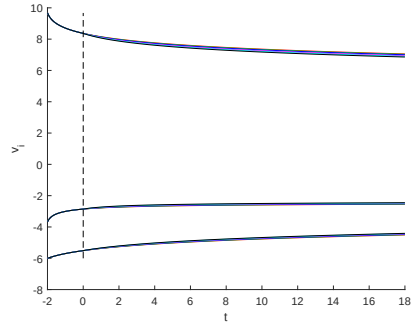

(C) Velocity v_i^τ with (2)

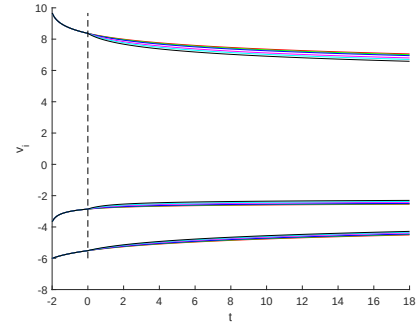

(D) Velocity v_i^τ with (3)

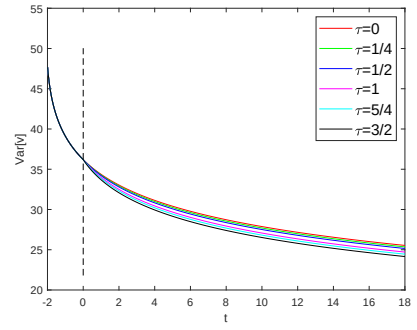

(E) Variance of v_i^τ with (2)

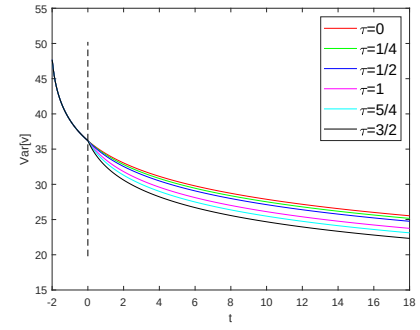

(F) Variance of v_i^τ with (3)

FIGURE 3. Simulation Results for $N = 3$: Time evolution of position(top), velcocity(middle) and variance(bottom) with two types of communication (2)(left) and (3)(right). Each line show the results with various time delays. History data and other parameter values are given in (18).

where $W_i(t)$ is the standard Wiener process (or Brownian motion). As assumed in $\mathbf{CS}(\tau)$, let N be the number of assets. Thus, the spot evolution of the price process $S_i(t)$ is governed by the market's expected return $x_i(t)$, volatility $v_i(t)$, and the geometric Brownian motion for $i = 1, ..., N$. Since $\dot{x}_i(t) = v_i(t)$, modeling the

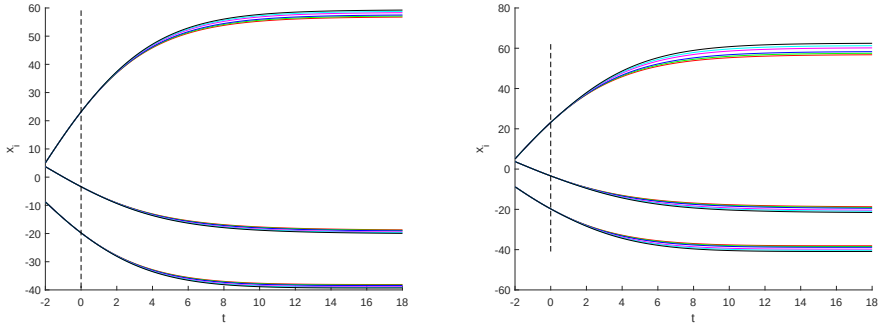

(A) Position x_i^τ with (2)

(B) Position x_i^τ with (3)

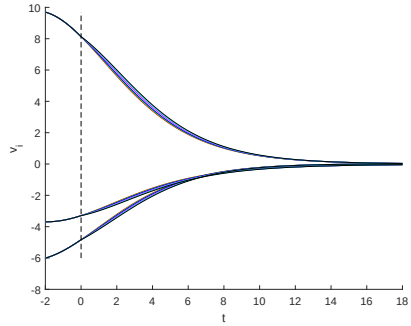

(C) Velocity v_i^τ with (2)

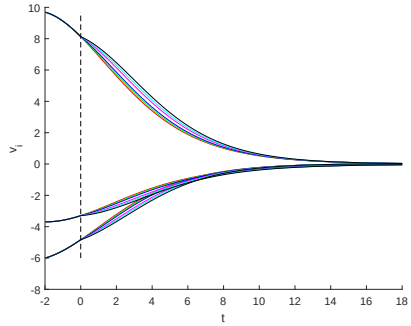

(D) Velocity v_i^τ with (3)

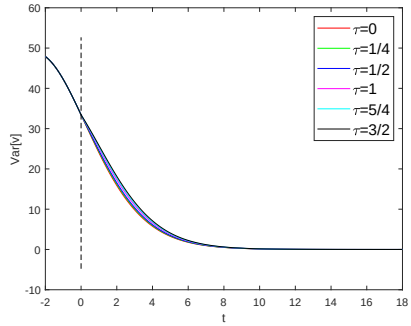

(E) Variance of v_i^τ with (2)

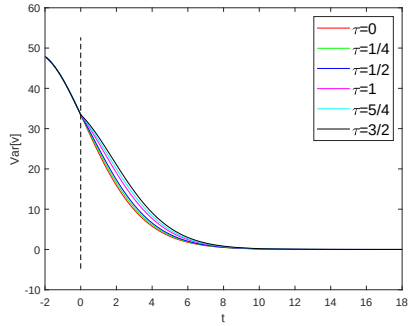

(F) Variance of v_i^τ with (3)

FIGURE 4. Simulation Results with $\gamma = -1$ in (4): Time evolution of position(top), velcocity(middle) and variance(bottom) with two types of communication (2)(left) and (3)(right). Each line show the results with various time delays. History data and other parameter values are given in (18).

dynamical system of $\dot{v}_i(t)$ is a key to understand both the expected return $x_i(t)$ and volatility $v_i(t)dW_i(t)$.

For simulation, we use daily closing prices of thirty companies ($N = 30$) that are listed on the Dow Jones Industrial Average Index (DJIA) as of May 22nd 2020. Our sample period starts from January 1st 2019 and ends on May 22nd, 2020. We

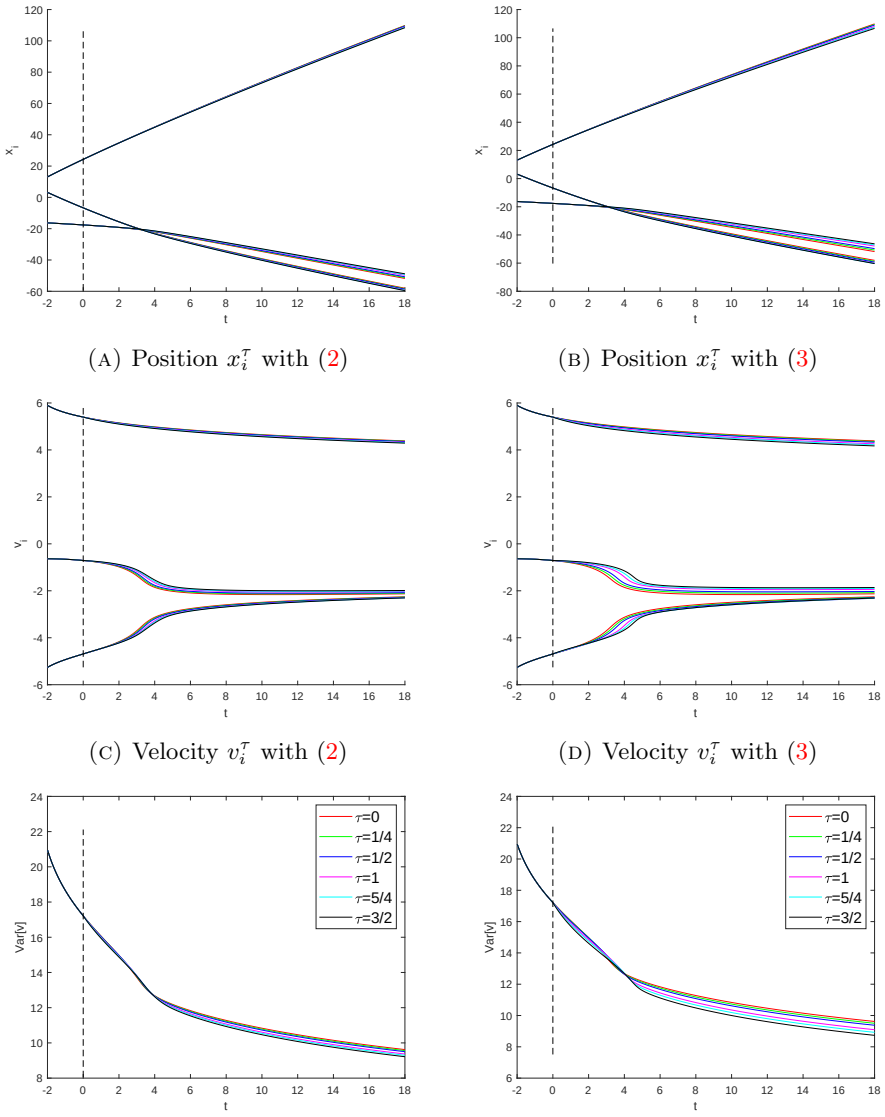

(A) Position x_i^τ with (2)

(B) Position x_i^τ with (3)

(C) Velocity v_i^τ with (2)

(D) Velocity v_i^τ with (3)

(E) Variance of v_i^τ with (2)

(F) Variance of v_i^τ with (3)

FIGURE 5. Simulation Results with $\gamma = -1$ in (4): Time evolution of position(top), velcocity(middle) and variance(bottom) with two types of communication (2)(left) and (3)(right). Each line show the results with various time delays. History data and other parameter values are given in (19), violating the condition (15).

set the time step size Δt as 2 days and the time delay τ as 1 day. For comparison, we consider the interaction kernel Ψ_{ij}^{τ} in (3). Denoting the predicted values of $\big(x_i^{\tau}(t+\Delta t), v_i^{\tau}(t+\Delta t)\big)$ by $\big(x_i^{\tau,pred}(t+\Delta t), v_i^{\tau,pred}(t+\Delta t)\big)$, we provide a discrete-version of Model $\mathbf{CS}(\tau)$ as follows:

$$\begin{cases} x_i^{\tau,pred}(t+\Delta t) = x_i^{\tau}(t) + \Delta t v_i^{\tau}(t), \\ v_i^{\tau,pred}(t+\Delta t) = v_i^{\tau}(t) + \frac{\Delta t \lambda}{N} \sum_{j=1}^{N} \Psi_{ij}^{\tau}(t)\big(v_j^{\tau}(t) - v_i^{\tau}(t)\big). \end{cases} \tag{21}$$

Now, the simulation procedure is summarized as follows: for each $i = 1, \cdots, N$, and $t = 0, 1, \cdots, T - \Delta t$,

- Step 1: Import realized data of $\big(x_i(s), v_i(s)\big)$ at $s = t - \tau$ and $s = t$.
- Step 2: Predict $v_i^{\tau,pred}(t+\Delta t)$ according to (21).

In Figure 6, we present our simulation results of $v_i^{\tau,pred}(t+\Delta t)$ and compare them with truly realized $v_{h,i}^{\tau}(t+\Delta t)$.

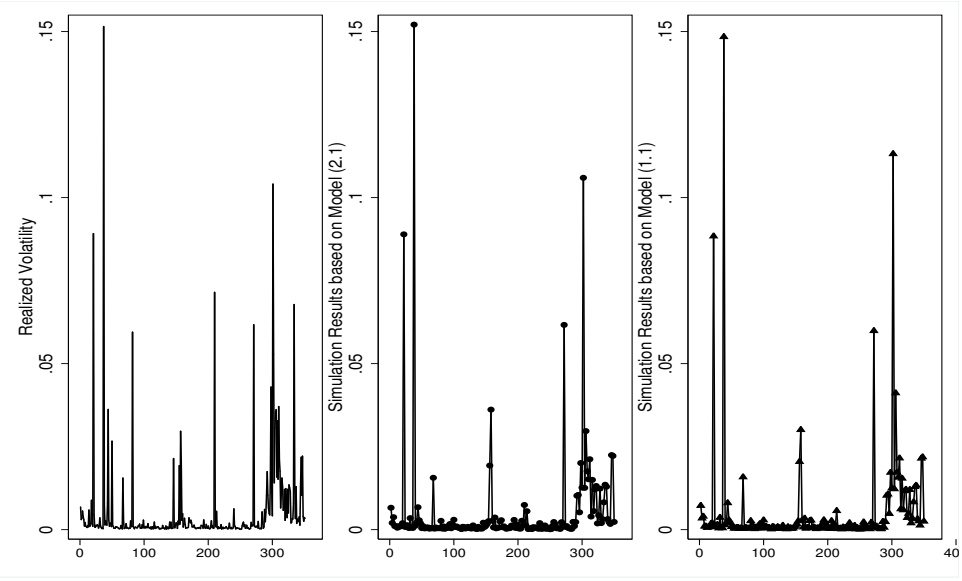

FIGURE 6. Comparison of real and simulated volatility data of General Electric (GE)
Left: Real volatility data
Center: Simulated data based on (1)
Right: Simulated data based on (21)
Note: Volatilities are drawn over the sample period. We use thirty firms listed on DJIA and $\lambda = 10$. See text for details of data sources and values of other parameters.

The model successfully predict real financial data, presenting a few noteworthy stylized facts about volatility dynamics. Particularly, simulated data exhibit volatility clustering (e.g., [14]), high/low volatilities continue for a while. The pattern is related to long memory (e.g., [12]) and propagating responses of an impulse with stochastic information arrival. We compare the results according to the mean squared errors and the simulated data's correlation with true data. The mean squared errors are computed as

$$\frac{1}{N}\frac{1}{T+1-\Delta t}\sum_{i=1}^{N}\sum_{t=0}^{T-\Delta t}\left(v_i^{\tau}(t+\Delta t)-v_i^{\tau,pred}(t+\Delta t)\right)^2,$$

where $v_i^{\tau}(t+\Delta t)$ indicate real volatility data.

We find that the simulation results of $\mathbf{CS}(\tau)$ show lower mean squared errors (1.316%) in forecasting the real data than them from (1) (1.328%). Particularly, the mean squared error of $\mathbf{CS}(\tau)$'s forecast is 1.254% whereas (1)'s is 1.4% in predicting real volatility of Exxon Mobile's return, which show the highest mean squared error among thirty volatility series during the sample period. Our model also provides better prediction than the EMH's prediction, of which the mean squared errors of 1.353%. Finally, $\mathbf{CS}(\tau)$ simulation results have the higher correlation (84.05%) with real data than the model (1) (82.14%).

However, $\mathbf{CS}(\tau)$ is somewhat limited in explaining the real volatility perfectly. For example, high picks around 310th day shown in real data are not fully predicted by simulations. Since $\mathbf{CS}(\tau)$ explains one asset's movement in the 30 assets network, the simulation shows its *relative* movement to others. If there is a macroeconomic shock to the entire market, then all assets' returns are moving in the similar way. Subsequently, simulated data plots are smoother than real points. Most notable peaks are around the start of COVID-19 pandemic, in which many firms were exposed to this unexpected shocks to macroeconomic conditions.

Despite more rooms to be discussed and investigated in the future study, our simulations show that financial data are relevant subjects to study the real application of **CS** system by their dynamics developed by the continuous communication/interaction. Notably, $\mathbf{CS}(\tau)$ provides understanding on one stock's price dynamics according to its relative movement to other 29 stocks in the same network. Such understanding is important in the optimal portfolio selection. If a stock's price movement is significantly different from other stocks, then it deserves attention for generating the minimum-risk portfolio. On the other hand, if all stocks in a basket are moving into the same direction, then its reaction to the shock may not contain valuable information.

Here, we provide more results from simulations based on real financial data. In this simulation, we focus on the results from $\mathbf{CS}(\tau)$. All simulations are conducted given the initial data in Jan., 1st 2019 through May. 2020. At every t, we predict $\Delta v = v_{t+1} - v_t$ and r_{t+1} according to the delayed interaction between asset return volatility v_t^i for $i = 1, \ldots, 30$. Other parameters are given same with the simulation of Figure 6.

Figure 7 show real volatility data and simulated data of two companies, CISCO and Walt Disney, with $\lambda = 10$, 30, and 100 for several companies that are listed on the DJIA. From Figure 7, we also find volatilities' comovement (e.g., [15, 30, 31]). Although the model generates a few negative volatility points, such negative values appear consistently in simulations of most of CS type volatility models. Particularly in $\mathbf{CS}(\tau)$'s simulation, as λ increases, the simulation results show more negative volatility points. The simulations with small λ's result higher forecasting power. The right choice of λ depends on initial data and other parameters like N and Ψ_{ij}. We leave this subject for the future study on the appropriate choice of λ.

REFERENCES

[1] J. A. Acebrón, L. L. Bonilla, C. J. P. Vicente, F. Ritort and R. Spigler, The Kuramoto model: A simple paradigm for synchronization phenomena, *Rev. Mod. Phys.*, **77** (2005), 137.

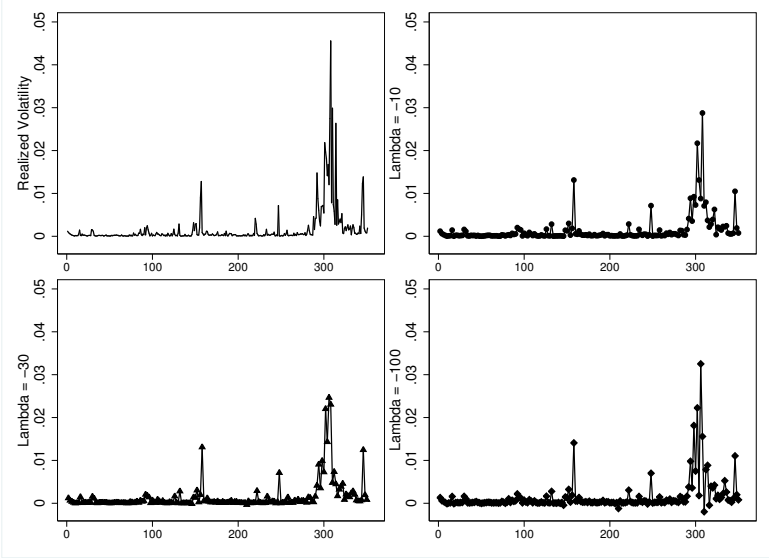

(A) Cisco Systems Inc. (CSCO)

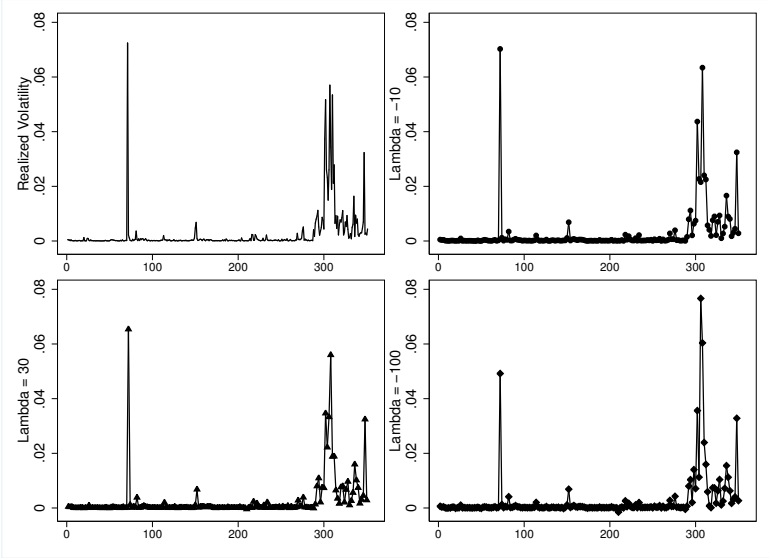

(B) Walt Disney Co. (DIS)

FIGURE 7. Historical and Simulated Volatilities with different λ: DIS and CSCO

Left-top: Real volatility data
Right-top: Simulated data based on $\mathbf{CS}(\tau)$ with $\lambda = -10$
Left-bottom: Simulated data based on $\mathbf{CS}(\tau)$ with $\lambda = -30$
Right-bottom: Simulated data based on $\mathbf{CS}(\tau)$ with $\lambda = -100$
Note: Volatilities are drawn over the sample period. We use thirty firms listed on DJIA. See text for details of data sources and values of other parameters.

[2] S. Ahn, H.-O. Bae, S.-Y. Ha, Y. Kim and H. Lim, Application of flocking mechanism to the modeling of stochastic volatility, *Math. Models Methods Appl. Sci.*, **23** (2013), 1603–1628.
[3] G. Albi, N. Bellomo, L. Fermo, S.-Y. Ha, J. Kim, L. Pareschi, D. Poyato and J. Soler, Vehicular traffic, crowds and swarms: From kinetic theory and multiscale methods to applications and research perspectives, *Math. Mod. Meth. Appl. Sci.*, **29** (2019), 1901–2005.
[4] G. Albi and L. Pareschi, Modeling of self-organized systems interacting with a few individuals: From microscopic to macroscopic dynamics, *Appl. Math. Lett.*, **26** (2013), 397–401.
[5] T. G. Andersen, Stochastic autoregressive volatility: A framework for volatility modeling, *Math. Fin.*, **42** (1994), 75–102.
[6] H.-O. Bae, S.-Y. Cho, J.-H. Kim and S.-B. Yun, A kinetic description for the herding behavior in financial market, *J. Stat Phys.*, **176** (2019), 398–424.
[7] H.-O. Bae, S.-Y. Cho, S.-H. Lee, J. Yoo and S.-B. Yun, A particle model for the herding phenomena induced by dynamic market signals, *J. Stat. Phys.*, **177** (2019), 365–398.
[8] H.-O. Bae, S.-Y. Ha, M. Kang, Y. Kim, H. Lim and J. Yoo, Time-delayed stochastic volatility model, *Phys. D: Nonlinear Phen.*, **430** (2022), 133088, 14 pp.
[9] H.-O. Bae, S.-Y. Ha, D. Kim, Y. Kim, H. Lim and J. Yoo, Emergent dynamics of the first-order stochastic Cucker-Smale model and application to finance, *Math. Methods Appl. Sci.*, **42** (2019), 6029–6048.
[10] H.-O. Bae, S.-Y. Ha, Y. Kim, S.-Y. Lee, H. Lim and J. Yoo, A mathematical model for volatility flocking with a regime switching mechanism in a stock market, *Math. Models Methods Appl. Sci.*, **25** (2015), 1299–1335.
[11] H.-O. Bae, S.-Y. Ha, Y. Kim, H. Lim and J. Yoo, Volatility flocking by cucker-smale mechanism in financial markets, *Asia-Pacific Fin. Mkts.*, **27** (2020), 387–414.
[12] R. T. Baillie, T. Bollerslev and H. O. Mikkelson, Fractionally integrated generalized autoregressive conditional heteroskedasticity, *J. Econom.*, **74** (1996), 3–30.
[13] N. Bellomo, H. Berestycki, F. Brezzi and J. Nadal, Mathematics and complexity in life and human sciences, *Math. Mod. Meth. Appl. Sci.*, **20** (2010), 1391–1395.
[14] T. Bollerslev, On the correlation structure of the generalize autoregressive conditional heteroscedastic process, *J. Time. Ser. Anal.*, **9** (1988), 121–131.
[15] T. Bollerslev and R. F. Engle, Common persistence in conditional variances, *Econometrica*, **61** (1993), 167–186.
[16] T. Bollerslev, R. F. Engle and J. M. Wooldridge, A capital asset pricing model with time-varying covariances, *J. Pol. Econ.*, **96** (1988), 116–131.
[17] J. A. Carrillo, Y.-P. Choi, P. B. Mucha and J. Peszek, Sharp conditions to avoid collisions in singular Cucker-Smale interactions, *Nonlinear Anal. Real World Appl.*, **37** (2017), 317–328.
[18] Y.-P. Choi and J. Haskovec, Cucker-Smale model with normalized communication weights and time delay, *Kinet. Relat. Models*, **10** (2017), 1011–1033.
[19] Y.-P. Choi and C. Pignotti, Emergent behavior of Cucker-Smale model with normalized weights and distributed time delays, *Netw. Heterog. Media*, **14** (2019), 789–804
[20] F. Cucker and S. Smale, Emergent behavior in flocks, *IEEE Trans. Automat. Control*, **52** (2007), 852–862.
[21] L. C. Davis, Modifications of the optimal velocity traffic model to include delay due to driver reaction time, *Phys. A: Stat. Mech. and its Appl.*, **319** (2003), 557–567.
[22] J.-G. Dong, S.-Y. Ha and D. Kim, Interplay of time-delay and velocity alignment in the Cucker-Smale model on a general digraph, *Discrete Contin. Dyn. Syst. Ser. B*, **24** (2019), 5569–5596.
[23] J.-G. Dong, S.-Y. Ha, D. Kim and J. Kim, Time-delay effect on the flocking in an ensemble of thermomechanical Cucker-Smale particles, *J. Differential Equations*, **266** (2019), 2373–2407.
[24] M. R. D'Orsogna, Y. L. Chuang, A. L. Bertozzi and L. S. Chayes, Self-propelled particles with soft-core interactions: Patterns, stability, and collapse, *Phys. Rev. Lett.*, **96** (2006), 104302.
[25] R. F. Engle, Autoregressive conditional heteroskedasticity with estimates of the variance of United Kingdom inflation, *Econometrica*, **50** (1982), 987–1007.
[26] S. Galam and J. Zucker, From individual choice to group decision-making, *Phys A: Stat. Mech. and its Appl.*, **287** (2000), 644–659.
[27] S. A. Gourley, J. H. So and J. H. Wu, Nonlocality of reaction-diffusion equations induced by delay: Biological modeling and nonlinear dynamics, *J. Math. Sci.*, **124** (2004), 5119–5153.
[28] S.-Y. Ha, K. Lee and D. Levy, Emergence of time-asymptotic flocking in a stochastic Cucker-Smale system, *Commun. Math. Sci.*, **7** (2009), 453–469.

[29] S.-Y. Ha, S. E. Noh and J. Park, Synchronization of Kuramoto oscillators with adaptive couplings, *SIAM J. Appl. Dyn. Syst.*, **15** (2016), 162–194.
[30] A. C. Harvey, E. Ruiz and E. Santana, Unobserved component time series models with ARCH disturbances, *J. Econom.*, **52** (1992), 129–157.
[31] G. A. Karolyi, A multivariate GARCH model of international transmission of stock returns and volatility: The case of United States and Canada, *J. Bus. Econ. Stat.*, **13** (1995), 11–25.
[32] Y. Kazmerchuk, A. Swishchuk and J. Wu, A continuous-time Garch model for stochastic volatility with delay, *Can. Appl. Math. Q.*, **13** (2005), 123–149.
[33] Y. N. Kyrychko and S. J. Hogan, On the use of delay equations in engineering applications, *J. Vib. Cont.*, **16** (2010), 943–960.
[34] S. M. Lenhart and C. C. Travis, Global stability of a biological model with time delay, *Proc. Amer. Math. Soc.*, **96** (1986), 75–78.
[35] Z. Li and X. Xue, Cucker-Smale flocking under rooted leadership with fixed and switching topologies, *SIAM J. Appl. Math.*, **70** (2010), 3156–3174.
[36] J. Lu, D. W. Ho and J. Kurths, Consensus over directed static networks with arbitrary finite communication delays, *Phys. Rev. E.*, **80** (2009), 066121.
[37] X. Lu, H. Zhang, W. Wang and K. L. Teo, Kalman filtering for multiple time-delay systems, *Automatica*, **41** (2005), 1455–1461.
[38] A. Martin and S. Ruan, Predator-prey models with delay and prey harvesting, *J. Math. Biol.*, **43** (2001), 247–267.
[39] S. Motsch and E. Tadmor, A new model for self-organized dynamics and its flocking behavior, *J. Stat. Phys.*, **144** (2011), 923–947.
[40] J. Park, H. J. Kim and S.-Y. Ha, Cucker-Smale flocking with inter-particle bonding forces, *IEEE Trans. Automat. Cont.*, **55** (2010), 2617–2623.
[41] M. R. Roussel, The use of delay differential equations in chemical kinetics, *J. Phys. Chem.*, **100** (1996), 8323–8330.
[42] J. Shen, Cucker-Smale flocking under hierarchical leadership, *SIAM J. Appl. Math.*, **68** (2007/08), 694–719.
[43] R. Sipahi, F. M. Atay and S. I. Niculescu, Stability of traffic flow behavior with distributed delays modeling the memory effects of the drivers, *SIAM J. Appl. Math.*, **68** (2008), 738–759.
[44] J. C. Sprott, A simple chaotic delay differential equation, *Phys. Lett. A.*, **366** (2007), 397–402.
[45] G. Stoica, A stochastic delay financial model, *Proc. Amer. Math. Soc.*, **133** (2005), 1837–1841.
[46] T. Vicsek, A. Cziròk, E. Ben-Jacob, I. Cohen and O. Shochet, Novel type of phase transition in a system of self-driven particles, *Phys. Rev. Lett.*, **75** (1995), 1226–1229.
[47] J. Zhang, J. Zhu and C. Qian, On equilibria and consensus of the Lohe model with identical oscillators, *SIAM J. Appl. Dyn. Syst.*, **17** (2018), 1716–1741.

Received for publication February 2022; early access June 2022.

E-mail address: hobae@ajou.ac.kr
E-mail address: chosy89@gnu.ac.kr
E-mail address: janeyoo@ajou.ac.kr
E-mail address: sbyun01@skku.edu